Fundamental combustion characteristics of laminar ultra-lean hydrogen/air flames

Nicolas Villenave, Seif Zitouni, Pierre Brequigny, Fabrice Foucher

Fundamental combustion characteristics of laminar ultra-lean hydrogen/air flames

Nicolas Villenave, Seif Zitouni, Pierre Brequigny, Fabrice Foucher
Univ. Orléans, INSA-CVL, PRISME, EA-4229, F-45072, Orléans, France

ABSTRACT

Ultra-lean hydrogen spark ignition engines is a rising solution to mitigate global warming. However, there is a lack of laminar burning velocity measurements under (ultra-)lean conditions at ambient pressure and temperature, which are crucial for validating or optimizing chemical models. Laminar flame speed and burnt Markstein lengths were measured at $P_u = 0.1$ MPa, $T_u = 303$ K and $\phi = 0.28$ - 0.6, using a constant-pressure spherical bomb. Thus, laminar flame speed showed reasonable agreement with existing literature datasets. However, the evaluated kinetic mechanisms tended to globally underpredict these values. In addition, significant decrease in burnt Markstein length was observed as the mixture becomes leaner, in accordance with the reduction in Lewis number in the ultra-lean region. Comparison between burnt Markstein length theoretical predictions and measured values shows that the model considering overall activation energy and thermal flame thickness highlights quantitative and qualitative agreement with present work.

1. Introduction

In order to limit the global median surface temperature increase by 2050, the European parliament announced the end of fossil-based engine commercialization for 2035. The use of green e-fuels to burn, such as hydrogen, is a part of the solution. Hydrogen combustion present many advantages such as wide flammability range, high burning rate, high flame temperature and no CO_2 emission. In comparison with diesel and gasoline-fueled internal combustion engines (ICEs), hydrogen internal combustion engines (H_2ICEs) offers a 10% higher brake and thermal efficiency. Thereby, H_2ICEs appears to be crucial to maintain road transport activities, especially for heavy-duty vehicules. Hydrogen spark ignition engines (H_2SIEs) are considered to operate at ultra-lean conditions with a fuel-air ratio (ϕ) below 0.4 to ensure near-zero nitric oxides (NO_x: NO, NO_2) and pollutant emissions (N_2O). Especially, NO_x are precursors to acid rain while N_2O holds a greater warming power than CO_2. Under these conditions, hydrogen combustion is still under study, especially because of abnormal combustion phenomenon such as misfire, knock, auto-ignition and pre-ignition. To better understand the complex behavior of ultra-lean hydrogen combustion, the experimental investigation of laminar burning velocity is needed to validate or improve detailed hydrogen chemical models under H_2SIEs conditions.

Laminar burning velocity (S_L^0) is an essential property, providing insights about the exothermicity and reactivity of the combustion process. Furthermore, it is a basis of turbulent combustion modeling for designing efficient and environmentally friendly combustion systems [1]. However, measuring the laminar flame speed of lean hydrogen mixtures is challenging due to the presence of thermo-diffusive instabilities. The Lewis number $Le = D_{th}/D_m$, characterizes the competition between thermal diffusion (D_{th}), which stabilizes the flame, and mass diffusion (D_m), which destabilizes it, across the flame front [1]. In the case of a lean hydrogen flame, Le is less than unity, indicating strong preferential diffusion and favoring the formation of cellular structures [1]. Only limited studies have conducted experimental measurements of laminar flame speeds for lean and ultra-lean hydrogen mixtures. Most part of these studies are not recent and do not use the most consistent extrapolation method defined later in this work. Taylor [2], Aung et al. [3], Kwon et al. [4], Lamoureux et al. [5], Verhelst et al. [6], Bradley et al. [7], Kuznetsov et al. [8] measured lean laminar flame speeds for lean and ultra-lean H_2/air flames at NTP conditions ($T_u = 300 \pm 3$ K and $P_u = 0.1 \pm 0.001$ MPa), using the linear-stretch extrapolation model, while Dayma et al. [9], Beeckmann et al. [10], Bauwens et al. [11] and Xie et al. [12] used the non-linear model. Noteworthily that leanest laminar flame speeds were measured using the linear model which is not suitable.

Thereby, this study aims to achieve several objectives concerning lean and ultra-lean outwardly propagating premixed spherical flames at NTP conditions: First, provide new laminar burning velocity measurements by employing the most relevant extrapolation method, as suggested by previous works, in order to fill the knowledge gap in peer-reviewed experimental datasets. Second, validate detailed hydrogen/air chemistry models and identify the most accurate kinetic mechanisms. Third, investigate the influence of stretch related behavior by validating already existing theoretical models that predict flame sensitivity to intrinsic instabilities.

2. Methods

2.1 Experimental methods

Flame speed propagation was measured using a stainless-steel constant-pressure spherical chamber fully described in [13]. The mixture is premixed using a four-blade fan before ignition and H_2, O_2, and N_2 were injected at the same time with a Coriolis Mass Flowmeter (deviation of 1%). Temperature and pressure were respectively measured with a K-type thermocouple ($\pm$ 1%) and a piezoelectric pressure transducer (deviation of 2%). For each condition, tests were repeated three times in order to minimize random errors. The flame front propagation is captured with an optical Z-type Schlieren method. The flame front evolution is recorded with a High-Speed Phantom V1610. Frames rate, snap-

Corresponding author: Nicolas Villenave
E-mail address: nicolas.villenave@univ-orleans.fr

shot dimension, and spatial resolution were respectively fixed to 19 000 fps, 768 x 768 pixels, and 0.091 mm/pixel. The recorded flame front propagation is processed by a MATLAB script using edge-detection algorithms.

2.2 Uncertainty quantification

Determination of experimental uncertainties is crucial to ensure accurate S_L^0. Uncertainty calculation follows the Moffat methodology [14]. The uncertainty for unstretched flame speed (S_b^0) is estimated by calculating temperature, pressure, imaging, statistical and radiation error:

$$U_{S_b^0}^{\pm} = \sqrt{\left(\frac{\Delta S_b^0}{S_b^0}\right)^2_{T,P,Rad} + \left(\frac{\Delta S_b^0}{S_b^0}\right)^2_{Img,Stat}} \quad (1)$$

Temperature and pressure error are estimated using Duva et al. [15] laminar burning velocity correlation. Radiation error is due to the radiative transfer from the outwardly propagating spherical flame. Yu et al. [16] correlation predicts an uncertainty of S_b^0 of 12.5% for the lowest ϕ down to 0.5% for the highest ϕ. Uncertainty linked to the imaging was estimated 2.5%. Finally the statistical error and is calculated as: $((\Delta S_b^0)/S_b^0)_{stat} = (t_{95\%}\sigma_{STD})/\sqrt{N}$ where $t_{95\%}$ is the value of the Student's t-distribution for $N = 3$ tests in a 95% confidence interval. Overall the error does not exceed 2.6%.

2.3 Theoretical specifications

Schlieren imaging allows to determine stretched flame speed $S_b = dR_f/dt$ from the burnt gas to the fresh gas. Stretch rate $K = 2S_b/R_f$ measures flame surface deformation (A) as it propagates and is purely produced by curvature effect in the case of an expanding spherical flame [1]. The unstretched flame speed (S_b^0) is determined through extrapolation methods. Wu and Law [17] empirically characterized the importance of K in the calculation of S_b^0 and Dowdy et al. [18] derived the linear stretch model (LS), considering low-stretched flame ($Le \approx 1$) $S_b = S_b^0 - L_bK$ where L_b is a phenomenological parameter measuring the flame sensitivity to stretch [1]. Frankel and Sivashinsky [20] mathematically determined the linear curvature model (LC) from Markstein study [19] considering thermal expansion and non-equidiffusion $S_b = S_b^0(1 - (2L_b)/R_f)$. Finally, based on Kelley and Law [21] study, the nonlinear model (NL) adapted for highly-stretched flame ($Le << 1$) $(S_b/S_b^0)^2 \ln(S_b/S_b^0)^2 = -2(L_bK)/S_b^0$. Then, through the different methods, S_b^0 can be determined by extrapolating the values of S_b at zero stretch ($K = 0$). Finally, laminar burning velocity is evaluated considering thermal expansion $S_L^0 = (\rho_b/\rho_u)\, S_b^0$ [1]. Both thermal and kinetic flame thickness are used to characterize flame front width. Thermal flame thickness is derived from temperature profile $\delta_{th} = (T_{ad} - T_u)/(dT/dx)_{max}$ while kinetic flame thickness depends on diffusion properties $\delta_k = \lambda/(\rho_u c_p S_L^0)$ [1]. Overall activation energy (E_a) is determined through the differential $E_a/R = \partial \ln(\rho_u S_L^0)/\partial\,(1/T_{ad})$ [1], with R the specific gas constant, and calculated by varying the unburnt temperature. Zel'dovich number corresponds to dimensionless activation energy and is important to determine as it is used in various models. Two different formulations are proposed. The classical formulation $\beta_1 = (E_a(T_{ad} - T_u))/(R\,T_{ad}^2)$ [1] and the Müller et al. [22] approximation $\beta_2 = (4\,(T_{ad} - T_u)/(T_{ad} - T^0)$ with T^0 the inner layer temperature. Lewis number using the effective formulation $Le_i = 1 + ((Le_{exc} - 1) + (Le_{def} - 1)A_i)/(1 + A_i)$ is calculated as in [36] with $A_i = 1 + \beta_i\,(1/\phi - 1)$. The Lewis number Le_{exc}/Le_{def} corresponds to the excedent/deficient reactant Lewis number $Le_{\mathrm{O}_2}/Le_{\mathrm{H}_2}$.

Chen et al. [23, 24] and Bechtold and Matalon [25] highlights relationships between Le, β and the burnt Makstein length L_b. On one hand, Chen and Wu derived an analytical model presented in to compute $L_{b,\mathrm{Chen}}$ with Eq. (2).

$$L_{b\,\mathrm{Chen,i}} = \left(\frac{1}{Le_i} - \left(\frac{\beta_i}{2}\right)\left(\frac{1}{Le_i} - 1\right)\right)\sigma\,\delta_k \quad (2)$$

with $i = 1$, 2, respectively to β_i formulation. On the other hand Bechtold and Matalon [25] deduced an other L_b formulation Eq. (2) as :

$$L_{b\,\mathrm{BM,i}} = \left(\frac{\gamma_1}{\sigma} + \left(\frac{\beta_i}{2}\big(Le_i - 1\big)\,\gamma_2\right)\right) \quad (3)$$

with: $\gamma_1 = (2\sigma)/(\sqrt{\sigma}+1)$ and $\gamma_2 = (4/(\sigma-1))(\sqrt{\sigma} - 1 - \ln((\sqrt{\sigma}+1)/2)$. Here γ_1 and γ_2 are parameters that depend on thermal expansion $\sigma = \rho_b/\rho_u$.

2.4 Numerical simulation

Given the simplified one-dimensional spherical geometry of the outwardly propagating flame and the absence of interactions between the flame and the combustion chamber on the experimental measurement ranges, it is possible to perform one-dimensional simulations. For this purpose, numerical simulations were conducted using the 1D freely-propagating premixed flat flame model with CANTERA software [26]. The employed numerical approach for resolution utilizes the finite difference method with a second-order upwind discretization scheme. Adaptive grid is employed to enhance convergence on a 20 cm grid length. Laminar burning velocity calculation takes into account the Soret effect and preferential diffusion, which becomes significant for H_2/air mixtures (Le < 1). Relative tolerance for steady-state problem and time stepping resolution were 1.0e-8 and 1.0e-15 respectively. Different old-to-recent relevant kinetic mechanisms were appraised to perform numerical simulation: Hong et al., Burke et al. [28], Kéromnès et al. [29], San Diego university [31], Alekseev et al. [30], Konnov et al. [32], Mei et al. [33] and Sun et al. [34].

3. Results and Discussion

Laminar burning velocity (S_L^0) were measured using different extrapolation models. Fig. 1 displays

the measured S_L^0 of (ultra-)lean H_2/air flames, alongside peer-reviewed datasets. Good agreement is exhibited between measured values and literature results, when the same extrapolation method is considered. However, values obtained using the NL are lower than those obtained with the LS and LC models due to the non-linear impact of stretch on flame propagation consideration for Le < 1. A comparison was also realized between the measured S_L^0 and various H_2/air appraised chemical models. It was observed that the overall simulations underestimates S_L^0 values except for Lamoureux et al. [5]. According to the simulation, S_L^0 better agreement was found with those extracted using the NL. Kinetic mechanisms proposed by Kéromnès et al. [29], Alekseev et al. [30], and Mei et al [33] exhibits best agreement with the measured data while Hong et al. [27] and Sun et al. [34] shows significant deviations.

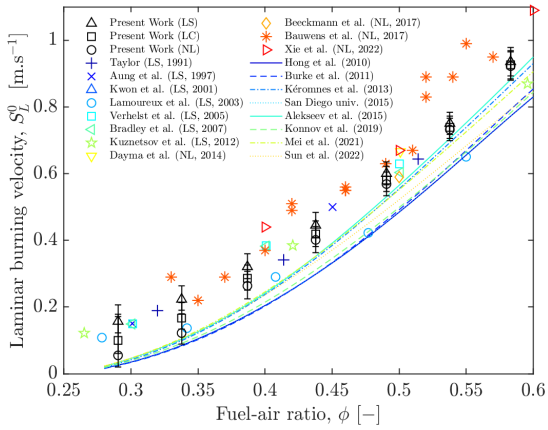

Fig. 1 Laminar burning velocity S_L^0 measurements under (ultra-)lean conditions at NTP. Comparison with peer-reviewed datasets at and appraised kinetic mechanisms at nominally similar conditions.

The burned Markstein length L_b serves as an indicator of flame's propensity to thermo-diffusional (TD) and Darrieus-Landau (DL) instabilities. In this work, measured L_b, displayed in Fig. 2, are compared with other measurements from the literature, for nominally identical conditions. Few experimental data are available for H_2/air mixtures at $\phi < 0.6$, especially using the NL model. Nevertheless, measured L_b using the LS model shows good agreement with those extracted from the previous works using the same method and underlines a linear decrease. Noteworthily, no specific comparison is available for L_b measured using the LC model. Finally, L_b measured using the NL equation are in fair agreement with those measured by Shu et al. [35] with the same extrapolation method. Markstein length is exponentially decreasing up to L_b = -25 mm, characterizing a highly thermo-diffusively unstable flame, indicating a decreasing Lewis number. It should be highlighted that authors provides first L_b values in the ultra-lean region $\phi < 0.4$.

In order to better understand this non-linear stretch-related behaviour, measured L_b from lean and ultra-lean H_2/air expanding flames were compared to theoretical L_b given by Chen [23] and Bechtold and Matalon [25] works. Fig. 3 depicts the comparison between $L_{b\,\mathrm{Chen},1}$, $L_{b\,\mathrm{Chen},2}$, $L_{b\,\mathrm{BM},1}$, $L_{b\,\mathrm{BM},2}$ and measured L_b. The burnt Markstein $L_{b\,\mathrm{BM},1}$, utilizing the classical β_1 Zel'dovich formulation, shows both quantitative and qualitative agreements with the presented L_b under lean and ultra-lean conditions, highlighting the significant impact of preferential diffusion on flame propagation. Other burnt Markstein length formulations, such as $L_{b\,\mathrm{Chen},1}$, $L_{b\,\mathrm{Chen},2}$, and $L_{b\,\mathrm{BM},2}$, demonstrate a reasonable qualitative agreement with the measured L_b, but tends to underpredict L_b at $\phi \approx 0.3$.

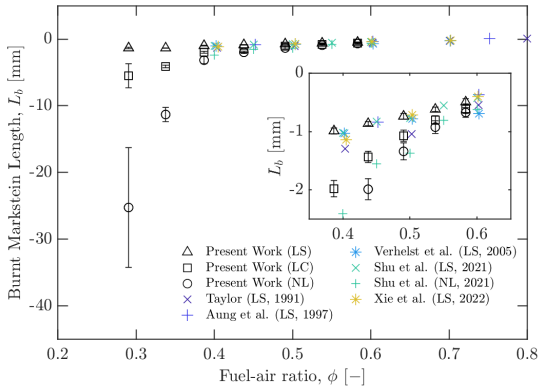

Fig. 2 Burnt Markstein lengths L_b measurements under (ultra-)lean conditions at NTP. Comparison with peer-reviewed datasets.

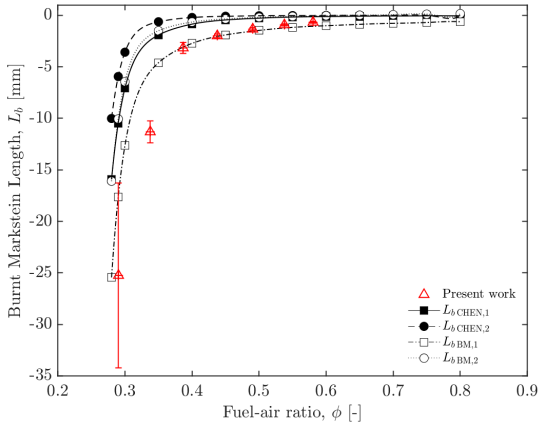

Fig. 3 Burnt Markstein lengths L_b measurements under (ultra-)lean conditions at NTP. Comparison with theoretical models.

To summarize, the Bechtold and Matalon Markstein model, using β_1 classic Zel'dovich formulation is giving a consistent prediction of ultra-lean premixed H_2/air spherical flames sensitivity to stretch. This is potentially due to two factors. First, the utilization of the thermal flame thickness δ_{th} definition. As a matter of fact, δ_{th} is preferable because as it is directly derived from the flame structure, since it is determined by the flame temperature profile and taking into account the preheat zone, transport

properties and heat release [1]. Secondly, the classic formulation of the Zel'dovich number β_1 is adapted as it is dependent of the overall activation energy, shifting drastically in the ultra-lean region, and embodying a change in the flame structure [1]. Finally, when H_2/air mixture becomes leaner, burnt Markstein length decreasing drastically, traducing a more sensitive flame to stretch-related behaviour.

4. Concluding Remarks

The constant pressure expanding spherical flame method was used to measure S_b^0 and corresponding L_b in (ultra-)lean H_2/air flames at NTP and using different extrapolation methods. Depending on the model, differences in S_L^0 occurs as the mixtures becomes leaner due to change in flame dynamics. Present work is in good agreement with peer-reviewed data and Alekseev et al. [30] and Mei et al. [33] chemical models displayed the best agreement with the measured S_L^0. Extrapolation equation are used to determine L_b and leaner mixtures results in a L_b decrease for the non-linear extrapolation model. A good agreement with extracted results from the literature is observed and consistent with Le behavior for (ultra-)lean H_2/air flames. In addition, Bechtold and Matalon [25] theoretic L_b model displayed a quantitative and qualitative agreement with measured L_b. It may be due to the overall activation energy consideration into the classic Zel'dovich formulation and the use of the thermal flame thickness in $L_{b\,\mathrm{BM},1}$.

References

[1] C.K. Law *Combustion Physics*, (2010).

[2] S. C. Taylor, *Ph.D. Thesis*, (1991).

[3] K. Aung, M. Hassan, G. Faeth, *Combust. Flame*, 109, (1997), 1-24.

[4] O. Kwon, G. Faeth, *Combust. Flame*, 124, (2001), 590-610.

[5] N. Lamoureux, N. Djebaıli-Chaumeix, C.-E. Paillard, *Exp. Therm. Fluid Sci.*, 27, (2003), 385-393.

[6] S. Verhelst, R. Woolley, M. Lawes, R. Sierens, *Proc. Combust. Inst.*, 30, (2005), 209-216.

[7] D. Bradley, M. Lawes, K. Liu, S. Verhelst, R. Woolley, *Combust. Flame*, 149, (2007), 162-172.

[8] M. Kuznetsov, S. Kobelt, J. Grune, T. Jordan, *Int J Hydrogen Energ*, 37, (2012), 17580-17588.

[9] G. Dayma, F. Halter, P. Dagaut, *Combust. Flame*, 161, (2014), 2235–2241.

[10] J. Beeckmann, R. Hesse, S. Kruse, A. Berens, N. Peters, H. Pitsch, M. Matalon, *Proc. Combust. Inst.*, 36, (2017), 1531–1538.

[11] C. Bauwens, J. M. Bergthorson, S. B. Dorofeev, *Int J Hydrogen Energ*, 42, (2017), 7691-7697.

[12] Y. Xie, M. E. Morsy, J. Li, J. Yang, *Fuel*, 327, (2022), 125149.

[13] B. Galmiche, F. Halter, F. Foucher *Combust. Flame*, 159, (2012), 3286-3299.

[14] R.J. Moffat, *Exp. Therm. Fluid Sci.*, 1, (1988), 3-17.

[15] B.C. Duva, E. Toulson, *Int J Hydrogen Energ*, 47, (2022), 9030-9044.

[16] H. Yu, W. Han, J. Santner, X. Gou, C.H. Sohn, Y. Ju, Z. Chen, *Combust. Flame*, 161, (2014), 2815-2824.

[17] C.K. Wu, C.K. Law, *Symposium on Combustion*, 20, (1985), 1941-1949.

[18] D.R. Dowdy, D.B. Smith, S.C. Taylor, A. Williams, *Symposium on Combustion*, 23, (1991), 325-332.

[19] G.H. Markstein, *Dynamics of curved fronts*, (1988), 413-423.

[20] M. Frankel, G. Sivashinsky, *Combust. Sci. Technol.*, 31, (1983), 131-138.

[21] A.P. Kelley, C.K. Law, *Combust. Flame*, 156, (2009), 1844-1851.

[22] U. Müller, M. Bollig, N. Peters, *Combust. Flame*, 108, (1997), 349-356.

[23] Z. Chen, M.P. Burke, Y. Ju, *Proc. Combust. Inst.*, 32, (2009), 1253-1260.

[24] Z. Chen, *Combust. Flame*, 157, (2011), 291-300.

[25] J. Bechtold, M. Matalon, *Combust. Flame*, 127, (2001), 1906-1913.

[26] D.G. Goodwin, H.K. Moffat, R.L Speth, 2018.

[27] Z. Hong, D.F. Davidson, R.K. Hanson, *Combust. Flame*, 158, (2011), 633-644.

[28] M.P. Burke, M. Chaos, Y. Ju, F.L. Dryer, S.J. Klippenstein, *Int J Chem Kinet*, 44, (2012), 444-474.

[29] A. Kéromnès, W.K. Metcalfe, K.A. Heufer, N. Donohoe, A.K. Das, C.-J. Sung, J. Herzler, C. Naumann, P. Griebel, O. Mathieu, *Comb. Flame*, 160, (2013), 995-1011.

[30] V.A. Alekseev, M. Christensen, A.A. Konnov, *Combust. Flame*, 162, (2015), 1884-1898.

[31] J. Gimenez-Lopez, C.T. Rasmussen, H. Hashemi, M.U. Alzueta, Y. Gao, P. Marshall, C.F. Goldsmith, P. Glarborg, *Int J Chem Kinet*, 48, (2016), 724-738.

[32] A.A. Konnov *Combust. Flame*, 203, (2019), 14-22.

[33] B. Mei, J. Zhang, X. Shi, Z. Xi, Y. Li, *Combust. Flame*, 231, (2021), 111472.

[34] W. Sun, Q. Zhao, H.J. Curran, F. Deng, N. Zhao, H. Zheng, S. Kang, X. Zhou, Y. Kang, Y. Deng, *Combust. Flame*, 245, (2022), 112308.

[35] T. Shu, Y. Xue, W. Liang, Z. Ren *Combust. Flame*, 226, (2021), 445-454.

[36] S. Zitouni, P. Brequigny, C. Mounaïm-Rousselle *Combust. Flame*, 253, (2023), 112786.